Journal of Engineering Mathematics **37:** 363–374, 2000.

Hydrodynamic influence on ship-hull vibration close to water bottom

Z. ZONG and K. Y. LAM
Institute of High Performance Computing, 89B Science Park Drive, #01-05/08, The Rutherford, Singapore Science Park I, Singapore 118261

Received 10 April 1998; accepted in revised form 26 April 1999

Abstract. The problem of a uniform ship-hull girder vibrating vertically close to water bottom is studied. A simple formula for the added mass is found by use of the method of matched asymptotic expansions. Results obtained from the present method and BEM are compared. They are in good agreement in the range considered here. The obtained added mass is used to predict the natural vibrations of a uniform beam vibrating close to water bottom. Numerical values show that the effects of shallow water are significant. The first- and second-order frequencies of the ship hull studied in this paper in deep water are about 1·4–3 times higher than those in shallow water.

Key words: hydrodynamic influence, ship hull vibration, shallow water, added mass.

1. Introduction

Structures like ship hulls vibrating in air and in water exhibit quite different vibration characteristics. The difference is due to hydrodynamic forces acting on the ship hull. It is well known that this hydrodynamic force can greatly reduce the natural frequencies of the ship hull.

Hydrodynamic influence on ship-hull vibration in water is expressed in terms of added mass. A ship hull vibrating in water brings the surrounding water in motion, which in turn exerts an opposing force on the hull. This additional force is required to accelerate the surrounding fluid. The effect is the same if an addition were made to the mass of the hull. This addition is hydrodynamic inertia mass called added mass. A vibrating ship then acts as if an added mass were attached. The added mass is of the same order as the ship mass and, thus, the natural frequencies of a ship hull are notably different from those of the same ship hull in air.

After the first documented systematic investigation of ship hull vibration by Schlick [1] in 1884, over 40 years elapsed before Lewis [2], in 1927, found that the water surrounding the ship has an important effect on the vibratory response. Until that time the significant differences between observed and calculated natural frequencies of the hull could not be explained. Lewis [3] presented a procedure to account for the effects of the fluid which is still by and large used today to analyse ship-hull-girder vibration [4]. In that method, the added mass of each section of the ship hull is found by use of a two-dimensional approach. Then, the added mass is multiplied by a 'J-factor' to account for three-dimensional flow influence.

Others have continued his work to investigate values of the J-factor using different types of bodies or extending the types of ship sections. These have notably been Lamb [5, 139–159], Landweber [6] and Vorus *et al*. [7]. A detailed review can be found in Daidola [4].

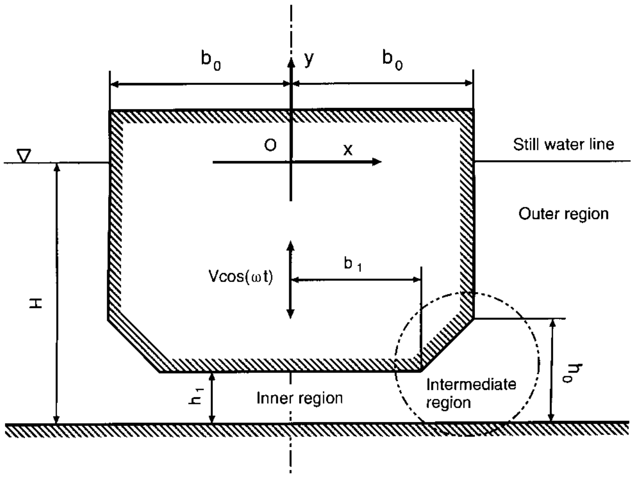

Figure 1. Problem definition.

Added mass depends on flow domain, such as water depth, flow-field boundaries, ship underwater shape and vibration modes. Thus, a ship hull in water of infinite water depth and finite water depth will show different vibration characteristics. At the present time, the added mass in water of infinite depth is used to predict ship-hull vibration. There are still only a few studies of ship-hull vibrations in shallow water, especially when the ship hull vibrates close to water bottom.

In this paper, the problem that a ship-hull girder vibrates vertically close to water bottom is studied. It is motivated by the increasing attention in recent years to accidents where grounding of large oil tankers resulted in severe oil spill. Cases have been found where oil spill occurred when tankers ran aground on relatively plane sloping bottoms. This is due to overall failure of the ship hull. This mode of failure seems not to have been discussed much [8]. A full fluid-structure interaction solution to the problem would require a lot of numerical effort and experimental verification, which are still beyond our capabilities at present time.

To simplify the problem as much as possible without losing essential features, we study a uniform beam of a typical ship section vibrating vertically close to water bottom and solve this problem in this paper by use of a simple model. In Section 2 a matched-asymptotic-expansion method introduced by Newman *et al.* [9] is used to find the added mass of a section vibrating vertically. A simple formula for the added mass is derived. The numerical values obtained from the present method and from BEM are compared. They are in good agreement in the range considered here.

In Section 3 the natural vibrations of a uniform beam of a typical ship section is studied with hydrodynamic influence included. Section 4 gives some numerical examples, which show that the shallow water influence is significant. The first- and second-order natural frequencies are reduced by a factor ramping from 1·4 compared with those of the same ship vibrating in deep water.

2. Added mass close to water bottom

Consider a two-dimensional cylinder with a typical U-shaped section as shown in Figure 1. The water depth is H and the gap between ship and water bottoms is h_1. Typically, $\varepsilon =$

$h_1/H \leqslant 0{\cdot}2$, which is assumed small throughout this paper. It is further assumed that $(b_0 - b_1)/H = O(\varepsilon)$, $(h_0 - h_1)/H = O(\varepsilon)$ and $(b_0 - b_1)/(h_0 - h_1) = O(1)$. The fluid domain is D, bounded by the free surface at $y = 0$, the body surfaces and the bottom surface at $y = -H$. The cylinder oscillates with the vertical velocity $\mathfrak{Re}\{V\,\mathrm{e}^{\mathrm{i}\omega t}\}$, where $\mathrm{i} = \sqrt{-1}$. With the usual assumption of irrotational flow, and small amplitudes of motion, the fluid velocity is given by the gradient of a velocity potential $\phi(x, y; t) = \mathfrak{Re}\{\varphi(x, y)\,\mathrm{e}^{\mathrm{i}\omega t}\}$, which satisfies

$$\nabla^2\varphi(x, y) = 0, \quad (x, y) \in D, \tag{1}$$

$$\frac{\partial\varphi}{\partial y} - \nu\varphi = 0, \quad y = 0, \quad \nu = \omega^2/g, \tag{2}$$

$$\left.\frac{\partial\varphi}{\partial n}\right|_{\text{on body surface}} = V_n, \qquad \frac{\partial\varphi}{\partial y} = 0, \quad y = -H, \tag{3,4}$$

$$\lim_{x\to\pm\infty} \mathfrak{Re}\left(\frac{\partial\varphi}{\partial x} \mp \mathrm{i}\nu\varphi\right) = 0, \tag{5}$$

where V_n is the normal velocity of the body surface and g is the gravity acceleration. Based on the fact that ε is a small quantity, the fluid domain can be divided into three regions:

1: Internal region $D_1 : |x| < b_1$ and $|y + H|/h_1 = O(1)$;

2: Intermediate region $D_2 : ||x| - b_0| = O(h_1)$ and $|y + H|/h_1 = O(1)$;

3: External region $D_3 : |x| > b_0$ and $h_1/y = O(\varepsilon)$.

The above division allows us to use a matched-asymptotic-expansion method to solve the problem.

The flow in the ‘internal region’ bounded by the narrow gap between the ship and water bottoms is first considered. Suppose the internal region potential is $\varphi_1(x, y)$, which satisfies

$$\nabla^2\varphi_1(x, y) = 0, \quad (x, y) \in D_1, \tag{6}$$

$$\left.\frac{\partial\varphi_1}{\partial y}\right|_{y=-H+h_1} = V, \qquad \left.\frac{\partial\varphi_1}{\partial y}\right|_{y=-H} = 0, \tag{7,8}$$

$$\varphi_1(-x, y) = \varphi_1(x, y). \tag{9}$$

The solution to the above problem [10] is

$$\varphi_1(x, y) = -\frac{V}{2h_1}[x^2 - (y + H)^2] + A_0 + \sum_{\ell=1}^{\infty} A_\ell \cosh\frac{\ell\pi x}{h_1} \cos\frac{\ell\pi(y + H - h_1)}{h_1}, \tag{10}$$

where the first term is the particular solution and the rest the homogenous solution. As $|x| \to b_1$, the last term is of order $\mathrm{e}^{1/\varepsilon}$ and tends to infinity as $\varepsilon \to 0$. Thus, $A_\ell = 0$ for $\ell \geqslant 1$. Meanwhile, as $|x| \to b_1$, $(y + h)^2/x^2 = O(\varepsilon^2)$. The outer expansion of the internal solution is then

$$\varphi_1^{(o)} = -\frac{V}{2h_1}x^2 + A_0. \tag{11}$$

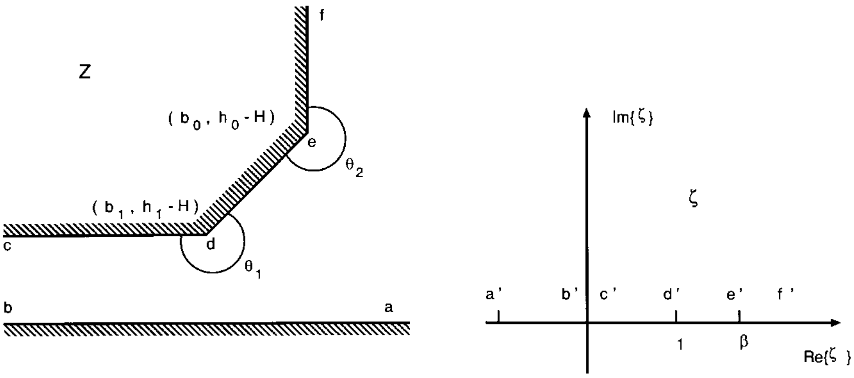

Figure 2. Schwarz–Christoffel transformation.

The above equation shows that the flow in the x-direction dominates the flow in the y-direction and the flow in the y-direction is negligible for the outer expansion solution.

The intermediate region refers to the neighborhood of point $(b_0, -H)$, in which $(y + H)/h_1 = O(1)$ as shown in Figure 2. In this figure, the section shape is defined by $\theta_1 = \pi/n + \pi$ and $\theta_2 = \pi/2 - \pi/n + \pi$, where n is arbitrary. Define complex co-ordinates $Z = x + \mathrm{i}y$. The flow is equivalent to that where the fluid flows into or out of the ‘narrow gap’ in an infinite domain. To find the potential in this region, a Schwarz–Christoffel transformation is used to map the flow in the Z-plane into the point source flow in the ζ-plane. In Figure 2, points a, b, c, d, e and f in the Z-plane are mapped to their counterparts a', b', c', d', e' and f' in the ζ-plane. The required transformation function is (see Appendix)

$$Z = b_1 + \mathrm{i}(h_1 - H) - \frac{\mathrm{i}h_1}{\pi\beta^{1/2-1/n}} \int_1^{\zeta} \frac{(\zeta - 1)^{1/n}(\zeta - \beta)^{1/2-1/n}}{\zeta}\,\mathrm{d}\zeta, \tag{12}$$

where β is the point in the ζ-plane corresponding to the point $(b_0, h_0 - H)$ in the Z-plane. If we define $t_0 = \sqrt{(b_0 - b_1)^2 + (h_0 - h_1)^2}$, β is determined by the following equation derived from Equation (12)

$$\pi\beta^{1/2-1/n} t_0 = h_1 \int_1^{\beta} \frac{(\zeta - 1)^{1/n}(\beta - \zeta)^{1/2-1/n}}{\zeta}\,\mathrm{d}\zeta. \tag{13}$$

We can also change the above equation into an algebraic equation for β, for which can not give an explicit expression for β and thus is omitted here. Once n is given, we can find β from Equation (13). For example, if the section is rectangular, then $n = 2$ and from Equation (13), $\beta = 1$. Generally, numerical methods are needed to solve the above eqution in order to find the corresponding β for given n. In Figure 3, the β values for $n = 3, n = 4$ and $n = 6$ are given with h_1/t_0 as abscissa and $h_1/\beta^{1/2-1/n}$ as ordinate. As can be seen later, the quantity $h_1/\beta^{1/2-1/n}$ appears in the final formula for the added mass and is selected as the ordinate here.

In the Appendix we give the asymptotic expansion for $\zeta \to \infty$

$$\zeta = \left(\frac{\pi Z\beta^{1/2-1/n}}{2\mathrm{i}h_1}\right)^2, \tag{14}$$

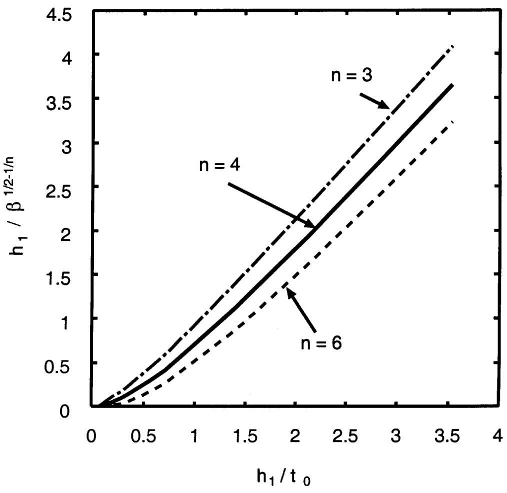

Figure 3. Relationship between β and n.

and the asymptotic expansion as $\zeta \to 0$

$$Z = b_1 + \frac{h_1}{\pi}(\log \zeta + K), \quad \text{where} \quad K = \left(\frac{1}{2} - \frac{1}{n}\right)\frac{1}{\beta} + \frac{1}{n}. \tag{15}$$

The flow in the ζ-plane is a point-source flow with strength Q at the origin point, of which the complex potential is

$$W(\zeta) = \frac{Q}{2\pi}\log \zeta + C, \tag{16}$$

where Q and C are to be found through matching. The outer expansion follows as $\zeta \to \infty$

$$\varphi_2^{(o)} = \mathfrak{Re}\{W|_{\zeta\to\infty}\} = \frac{Q}{\pi}\log\frac{\pi r \beta^{1/2-1/n}}{2h_1} + C, \tag{17}$$

where $r = \sqrt{(x-b_0)^2 + (y+H)^2}$. The inner expansion follows as $\zeta \to 0$

$$\varphi_2^{(i)} = \mathfrak{Re}\{W|_{\zeta\to 0}\} = \frac{Q}{2h_1}\left(x - b_1 - \frac{h_1}{\pi}K\right) + C. \tag{18}$$

In the external region, the vertical sides of the ship do not generate any disturbance. The only source to generate the disturbance is the periodical 'inhaling' and 'exhaling' water from the narrow gap between the ship and water bottoms. This disturbance is equivalent to a source with strength q at point $(b_0, -H)$, which is described by

$$\nabla^2\varphi_3(x, y) = 0, \quad (x, y) \in D_3, \tag{19}$$

$$\frac{\partial \varphi_3}{\partial y} - \nu\varphi_3 = 0, \quad y = 0, \nu = \omega^2/g, \tag{20}$$

$$\left.\frac{\partial \varphi_3}{\partial x}\right|_{|x|=b_0} = 0, \qquad \left.\frac{\partial \varphi_3}{\partial y}\right|_{y=-H} = 0, \tag{21, 22}$$

$$\lim_{x\to\pm\infty} \Re\mathfrak{e}\left(\frac{\partial\varphi}{\partial x} \mp \mathrm{i}\nu\varphi_3\right) = 0. \tag{23}$$

The solution to the above problem is given by Wehausen and Laitone [11, pp. 447–483]

$$\begin{aligned}
&\varphi_3(x, y)\\
&= q\left\{\frac{1}{m_0}\frac{m_0-\nu^2}{m_0H-\nu^2H+\nu}\cosh[m_0(y+H)]\cosh(m_0H)\sin[m_0|x-b_0|]\right.\\
&\quad\left.-\sum_{k=1}^{\infty}\frac{1}{m_k}\frac{m_k+\nu^2}{m_kH+\nu^2H-\nu}\cosh[m_k(y+H)\cos(m_kH)\exp[-m_k|x-b_0|]\right\}\\
&\quad+\mathrm{i}q\left\{\frac{1}{m_0}\frac{m_0-\nu^2}{m_0H-\nu^2H+\nu}\cosh[m_0(y+H)]\cosh(m_0H)\cos[m_0(x-b_0)]\right\},
\end{aligned} \tag{24}$$

where m_0 and m_k satisfy

$$m_0\tanh(m_0H) - \nu = 0 \quad \text{and} \quad m_k\tan(m_kH) + \nu = 0. \tag{25}$$

In this solution, the free-surface effects are taken into account. Generally speaking, the frequencies of the waves in oceans range from 0·04 – 2 Hz. Above 2 Hz, the wave effects can be neglected and the free-surface condition can be replaced by the high-frequency limit $\nu \to \infty$. On the other hand, the lowest natural frequencies of a typical ship range from 5 Hz to 10 Hz. Only in very special cases for supertankers may the lowest natural frequency be as low as 1 Hz. Here, we assume that wave effects are not important and that the free-surface condition can be replaced by $\varphi_3 = 0$, which we obtain from Equation (20) by letting $\nu \to \infty$. The corresponding solution can be obtained for $\nu \to \infty$ in Equation (24). Setting $\nu \to \infty$, we know that $m_0 \to \infty$ and $m_kH \to (k-1/2)\pi$ from Equation (25). Therefore, the first and the last terms in Equation (24) are zeros as $m_0 \to \infty$. Substituting m_k in Equation (24), we obtain the solution φ_3 in the limit of high frequency

$$\varphi_3(x, y) = -q\sum_{k=1}^{\infty}\frac{1}{m_kH}\cos(m_k\alpha)\,\mathrm{e}^{-m_k\gamma}, \tag{26}$$

where

$$\alpha = (y+H) \quad \text{and} \quad \gamma = |x-b_0|. \tag{27}$$

As $r = \sqrt{(x-b_0)^2+(y+H)^2} \to 0$, we obtain the inner expansion of φ_3

$$\begin{aligned}
\varphi_3^{(i)} &= -q\sum_{k=1}^{\infty}\left[\frac{1}{m_kH}\cos(m_kH\alpha)\,\mathrm{e}^{-m_kH\gamma} - \frac{1}{k\pi}\,\mathrm{e}^{-k\pi r/H}\right] - q\sum_{k=1}^{\infty}\frac{1}{k\pi}\,\mathrm{e}^{-k\pi r/H}\\
&= \frac{q}{\pi}\log(1-\mathrm{e}^{-\pi r/H}) - q\sum_{k=1}^{\infty}\left[\frac{1}{m_k}\cos(m_k\alpha)\,\mathrm{e}^{-m_k\gamma} - \frac{1}{k\pi}\,\mathrm{e}^{-k\pi r/H}\right]\\
&\sim \frac{q}{\pi}\log(\pi r/H) - \frac{q}{\pi}S,
\end{aligned} \tag{28}$$

where S is

$$S = \frac{1}{2}\sum_{k=1}^{\infty}\frac{1}{k(k-0{\cdot}5)} = 2\sum_{k=1}^{\infty}\frac{1}{2k(k-1)}$$

$$= 2\sum_{k=1}^{\infty}\left(\frac{1}{2k-1}-\frac{1}{2k}\right) = 2(1-\tfrac{1}{2}+\tfrac{1}{3}-\cdots) = 2\log 2. \tag{29}$$

Constants A_0, q, Q and C are to be determined by matching. Through the intermediate region to the external region, we have the matching condition

$$\varphi_3^{(i)} = \varphi_2^{(o)}, \tag{30}$$

which yields

$$Q = q \quad \text{and} \quad C = -\frac{q}{\pi}S + \frac{q}{\pi}\log\left[\frac{2h_1}{H\beta^{1/2-1/n}}\right]. \tag{31}$$

Another matching requirement, *i.e.*, $\partial\varphi_3^{(i)}/\partial r = \partial\varphi_2^{(0)}/\partial r$, turns out to give the same results as above, and thus is omitted here.

Through the intermediate and internal regions, we have

$$\varphi_2^{(i)} = \varphi_1^{(o)}, \quad \text{on } |x| = b_1, \tag{32}$$

$$\frac{\partial\varphi_2^{(i)}}{\partial x} = \frac{\partial\varphi_1^{(o)}}{\partial x}, \quad \text{on } |x| = b_1, \tag{33}$$

which yield

$$Q = -2Vb_1 \quad \text{and} \quad A_0 = -\frac{QK}{2\pi} + C + \frac{Vb_1^2}{2h_1}. \tag{34}$$

The hydrodynamic force on the body follows from the linearized Bernoulli's equation

$$P = \omega\rho\varphi|_{\text{on body surface}} = 2\omega\rho\left[\int_0^{b_1}\varphi_1\,\mathrm{d}x + \int_{b_1}^{b_0}\frac{\varphi_2(b_0-b_1)}{\sqrt{(b_0-b_1)^2+(h_0-h_1)^2}}\,\mathrm{d}x\right]. \tag{35}$$

Substituting φ_1 and φ_2 in the above equation, we have

$$\frac{P}{\pi\omega\rho V b_1^2} = \frac{2b_1}{3\pi h_1} + \frac{2K}{\pi^2} - \frac{4}{\pi^2}\left(1 + \frac{\sqrt{(b_0-b_1)^2+(h_0-h_1)^2}}{b_1}\right)\left(\log\frac{2h_1}{H\beta^{1/2-1/n}} - S\right). \tag{36}$$

The added mass m_a is defined by

$$\frac{m_a}{\omega V\pi\rho b_0^2} = \frac{b_1^2}{b_0^2}\left[\frac{2b_1}{3\pi h_1} + \frac{2K}{\pi^2} - \frac{4}{\pi^2}\left(1 + \frac{\sqrt{(b_0-b_1)^2+(h_0-h_1)^2}}{b_1}\right) \times \left(\log\frac{2h_1}{H\beta^{1/2-1/n}} - S\right)\right]. \tag{37}$$

Table 1. Constants in the eigen-solutions.

Mode i	1	2	3	4	5
e_i	3·56	9·82	19·24	31·81	47·52
$q_i L$	4·730	7·8532	10·9956	14·137	17·2788
R_i	0·9825	1·008	0·99997	1·0000	0·999999

3. Ship-vibration prediction

Consider a uniform beam of the section shown in Figure 1 as a simplified model of the ship hull. The moment of inertia of this section is I and the elastic modulus E. The mass per unit length is m and the added mass m_a. Let $M = m + m_a$ be the virtual mass per unit ship length. The ship length is L.

The vertical flexural displacement is assumed to be $W(x, t) = y(x)\cos(\omega t)$. When the effects of rotary inertia and shear deflection of the beam are assumed small, which is a reasonable assumption in ship-vibration analysis in most cases, the vibratory response is described by the following Euler equation

$$EI\frac{\mathrm{d}^4 y(x)}{\mathrm{d}x^4} - M\omega^2 y(x) = 0. \tag{38}$$

In general, the boundary condition for the above equation in ship vibration analysis is free-free. The solution for a free-free beam is

$$\text{natural frequency} \quad \omega_i = 2\pi e_i\sqrt{\frac{EI}{ML^4}}, \tag{39}$$

$$\text{eigen mode} \quad \psi_i(x) = \cosh(q_i x) + \cos(q_i x) - R_i(\sinh(q_i x) + \sin(q_i x)), \tag{40}$$

where e_i, q_i and R_i for the first five orders are given in Table 1.

From the above equation we conclude that, for a uniform beam, the added mass does not come into the eigenmode equations and thus does not have any influence on the vibration modes. This is not true for a nonuniform beam. A better understanding of the hydrodynamic influence on the vibration modes will come from a numerical analysis.

4. Numerical results and analysis

The numerical values of the added mass for a rectangular section ($n = 2$) are predicted by Equation (37) and plotted in Figure 4 with h_1/H as abscissa and the nondimensional added mass as ordinate. The ratio h_1/H ranges from 0·01 to 0·5. Because the differences of the numerical values at the two ends are dramatic a logarithm scale is used. To show the influence of another important parameter b_0/H, three curves for $b_0/H = 1{\cdot}0, 0{\cdot}5$ and 0·25 are also given in the figure.

Table 2. Definition of U-shaped sections.

b_0/H	b_1/H	h_0/H	t_0/H
1·0	0·1	0·1	0·1414
0·5	0·1	0·1	0·1414
0·25	0·05	0·05	0·0707

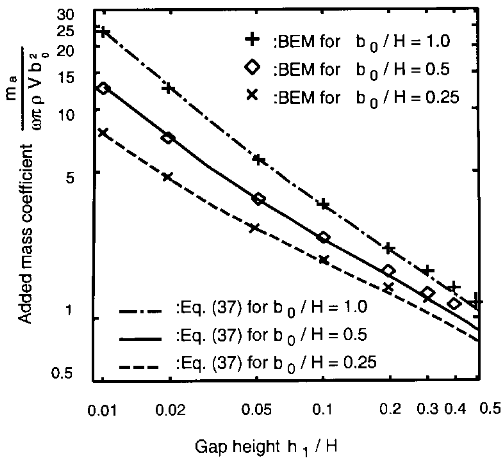

Figure 4. Added mass obtained from the present method and BEM for rectangular sections ($n = 2$).

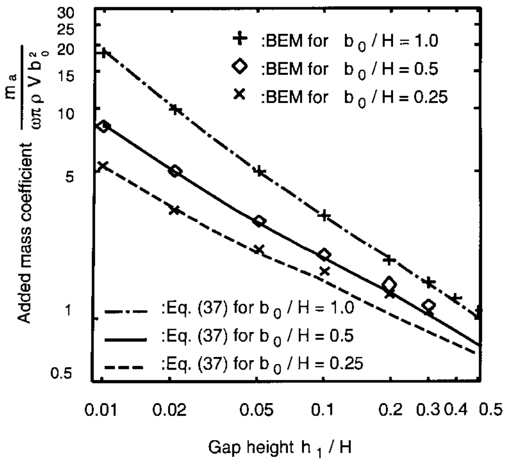

Figure 5. Added mass obtained from the present method and BEM for U-shaped sections ($n = 4$).

To check the validity of Equation (37), the numerical results obtained from BEM [12 pp. 347–352] for the same sections and fluid domains are also given in Figure 4. To minimize the numerical-approximation errors in BEM, the boundary is first discretized by N_1 elements (not necessarily uniform) and we obtain the added mass $m_a^{(1)}$. In the second round of computations, the boundary is descritized by $N_2 = 4N_1$ elements and we obtain the numerical value $m_a^{(2)}$. If the relative error $(m_a^{(2)} - m_a^{(1)})/m_a^{(2)} < 2\%$, then $m_a^{(2)}$ is regarded as the true value. Otherwise, the computation is continued until the relative error is smaller than the specified value. When $h_1/H \geqslant 0{\cdot}15$, the convergence of the BEM result to the true value is very fast. When $h_1/H \leqslant 0{\cdot}1$, especially when $h_1/H \approx 0{\cdot}01$, the convergence to the true value is very slow, and many boundary elements have to be used. This is due to the rapid flow variation in the narrow gap between the ship and the water bottoms.

Generally speaking, the agreement between the results obtained from BEM and the present method are good for smaller values of h_1/H. If the BEM results are taken as the true values, and the relative errors between the two methods are kept within 5%, it is observed from Figure 4 that Equation (37) is valid if $h_1/H \leqslant 0{\cdot}4$ for $b_0/H = 1{\cdot}0$, $h_1/H \leqslant 0{\cdot}2$ for $b_0/H = 0{\cdot}5$, and $h_1/H \leqslant 0{\cdot}1$ for $b_0/H = 0{\cdot}25$. In other words, Equation (37) is valid if $h_1/b_0 \leqslant 0{\cdot}4$. This value is higher than expected, because, at the beginning of the paper, h_1/b_1 was assumed to be smaller than 0·1–0·2.

In Figure 5, we consider a U-shaped section ($n = 4$) with 45° corner. The section shapes for the three different values of b_0/H are defined in Table 2. The values of the added mass for the three cases show a tendency similar to that of Figure 4. In this example, however, Equation (37) is valid if $h_1/b_1 \leqslant 0{\cdot}3$–$0{\cdot}4$, if 5% relative errors are used as before.

To study the hydrodynamic influence on the natural vibration, a uniform beam of length $L = 100$ meters is considerd. One ship section is rectangular with width $2b_0 = 20$ meters and draft $D = 8$ meters. Another section considered is U-shaped with 45° corners. Its width and draft are the same as the rectangular one. The other section parameters are: $b_1 = 9$ meters and $h_0 = h_1 + 1$ meters, where h_1 is a variable.

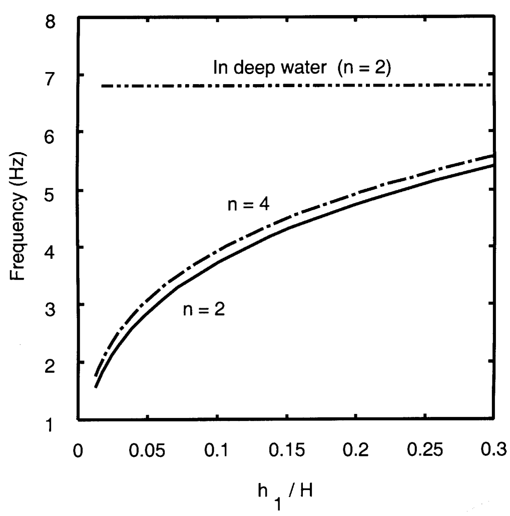

Figure 6. The first-order natural frequency for the uniform beam.

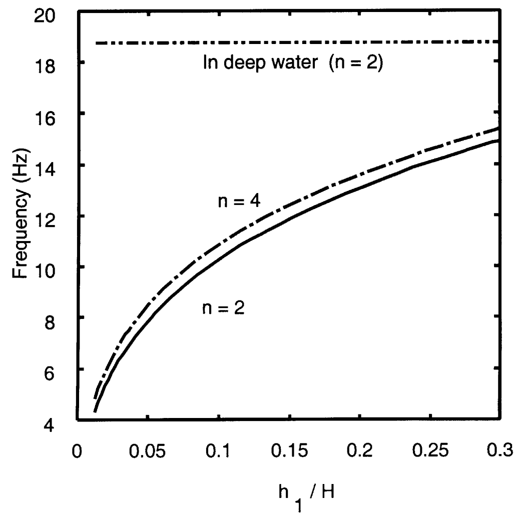

Figure 7. The second-order natural frequency for the uniform beam.

Figures 6 and 7 present the first- and second-order natural frequencies of the above beam models as predicted by Equation (39). The natural frequencies are increasing functions of h_1/H with the frequencies in deep water as the asymptotic line. From Figures 6 and 7, it is estimated that the first- and second-order frequencies in deep water are about three times higher than those close to water bottom for $h_1/H = 0{\cdot}01$ and about 1·4 times higher for $h_1/H = 0{\cdot}3$. Because three-dimensional effects are neglected, the frequency differences predicted above are somewhat over-estimated. Even so, these values still show clearly that the influence of a shallow-water bottom on ship-hull vibrations is significant. For higher-order natural frequencies, which exhibit a similar tendency, are not given here.

One comment should be given on the two-dimensional assumption on added mass. As is known, this assumption may overestimate added-mass values. The J-factor introduced in the introduction is, however, near to 1 for lower-order vibrations in many cases. Especially for a uniform beam, a two-dimensional flow can give a good prediction. Even so, further studies are needed to clarify three-dimensional effects on the added mass.

5. Conclusion

Motivated by the increasing attention that has been given in recent years to accidents where grounding of large oil tankers resulted in severe spill, the problem of a ship-hull girder vibrating vertically close to water bottom has been studied in this paper.

A simple formula for the added mass of a section vibrating vertically was found by means of the method of matched asymptotic expansions. The numerical values obtained from the present method and BEM have been compared. They were seen to be in good agreement in the range considered here.

With the hydrodynamic influence included, the natural frequencies of a uniform beam, which vibrates vertically in shallow water with different gaps between the ship and water bottoms, have been given. Numerical values showed that the effects of shallow water are significant. The frequencies in deep water are about 1·4–3 times higher than those in shallow water, which are more likely to cause the overall failure of the ship-hull girder.

Despite the assumptions introduced in this paper, it is safe to conclude that the influence of shallow water on ship-hull vibration, especially the natural frequencies, are significant and should be considered in the design stage.

Appendix. Schwarz–Christoffel transformation

By means of a Schwarz–Christoffel transformation the physical region in the Z-plane can be mapped to the upper half of the ζ-plane. As Figure 2 illustrates, the points a, b, c, d, e and f in the Z-plane are mapped to their counterparts a', b', c', d', e' and f' in the ζ-plane. Referring to Figure 2 with $\theta_1 = \pi/n + \pi, \theta_2 = \pi/2 - \pi/n + \pi$ where n is arbitrary, we have the Schwarz–Christoffel transformation as follows

$$Z = A \int \frac{(\zeta - 1)^{1/n}(\zeta - \beta)^{1/2-1/n}}{\zeta}\, \mathrm{d}\zeta + B. \tag{A.1}$$

Noting that in this case

$$\zeta = 0 \quad \text{for } Z = -\infty, \quad \text{and} \quad \zeta = 1 \quad \text{for } Z = b_1 + i(h_1 - H),$$

we have

$$Z = -A\mathrm{i} \int \frac{(\zeta - 1)^{1/n}(\zeta - \beta)^{1/2-1/n}}{\zeta}\, \mathrm{d}\zeta + b_1 + \mathrm{i}(h_1 - H). \tag{A.2}$$

In order to find A, let us consider the change in Z as we pass from b to c. In the Z-plane clearly $\Delta Z = \mathrm{i}h_1$ whereas in the ζ-plane moving from b' to c' corresponds to passing through a semicircle $c_r : \zeta = r\,\mathrm{e}^{\mathrm{i}\lambda}$ (λ going from π to 2π).

$$\begin{aligned}\Delta Z &= -A\mathrm{i} \int_{c_r} \frac{(\zeta - 1)^{1/n}(\zeta - \beta)^{1/2-1/n}}{\zeta}\, \mathrm{d}\zeta \approx -A\mathrm{i} \int_{c_r} \frac{(-1)^{1/n}(-\beta)^{1/2-1/n}}{\zeta}\, \mathrm{d}\zeta \\ &= \int_{\pi}^{2\pi} \frac{r\,\mathrm{e}^{\mathrm{i}\lambda}}{r\,\mathrm{e}^{\mathrm{i}\lambda}} \mathrm{i}\mathrm{d}\lambda \beta^{1/2-1/n} = \pi A\mathrm{i}\beta^{1/2-1/n}.\end{aligned}$$

Comparing both values from Δz we have

$$A = \frac{h_1}{\pi\beta^{1/2-1/n}},$$

and Z is given by

$$Z = b_1 + \mathrm{i}(h_1 - H) - \frac{\mathrm{i}h_i}{\pi\beta^{1/2-1/n}} \int_1^{\zeta} \frac{(\zeta - 1)^{1/n}(\zeta - \beta)^{1/2-1/n}}{\zeta}\, \mathrm{d}\zeta. \tag{A.3}$$

Imposing the condition that $Z = b_0 + \mathrm{i}(h_0 - H)$ for $\zeta = \beta$, we can find β from the above equation for given n. The approximation for $\zeta \to 0$ is

$$\begin{aligned} Z &= b_1 + \mathrm{i}(h_1 - H) - \frac{\mathrm{i}h_1}{\pi\beta^{1/2-1/n}} \int_1^{\zeta} \frac{\mathrm{i}\beta^{1/2-1/n}(1-\zeta)^{1/n}(1-\zeta/\beta)^{1/2-1/n}}{\zeta}\,\mathrm{d}\zeta \\ &= b_1 + \mathrm{i}(h_1 - H) + \frac{h_1}{\pi} \int_1^{\zeta} \sum_{l=0}^{\infty} C_{1/n}^{l}(-\zeta)^l \sum_{m=0}^{\infty} C_{1/n}^{m}(-\zeta/\beta)^m \,\mathrm{d}\zeta/\zeta \\ &\approx b_1 + \mathrm{i}(h_1 - H) + \frac{h_1}{\pi}(\log\zeta + K), \end{aligned} \tag{A.4}$$

where $K = (1/2 - 1/n)/\beta + 1/n$ is the integration constant.

The approximation for $\zeta \to \infty$ is

$$Z = b_1 + \mathrm{i}(h_1 - H) - \frac{\mathrm{i}h_1}{\pi\beta^{1/2-1/n}} \int_1^{\zeta} \frac{\zeta^{1/n}\zeta^{1/2-1/n}}{\zeta}\,\mathrm{d}\zeta \approx \frac{-2\mathrm{i}h_1\zeta^{1/2}}{\pi\beta^{1/2-1/n}}. \tag{A.5}$$

References

1. O. Schlick, On the vibration of stream vessels. *Inst. of Naval Architects* 5 (1884) 1–16.
2. F. M. Lewis, Vibration and engine balance in diesel ships. *Trans. SNAME* 35 (1927) 259–286.
3. F. M. Lewis, The inertia of the water surrounding a vibrating Ship. *Trans. SNAME* 37 (1929) 1–20.
4. J. C. Daidola, Natural vibrations of beams in a fluid with applications to ships and other marine structures. *Trans. SNAME* 92 (1984) 331–351.
5. H. Lamb, *Hydrodynamics*, 6th edn. New York: Dover Publications (1932) 738 pp.
6. L. Landweber, Vibration of a flexible cylinder in a fluid. *J. Ship Res.* 13 (1967) 143–150.
7. W. S. Vorus and S. Hylarides, Hydrodynamic added-mass matrix of vibrating ship based on a distribution of hull surface sources. *Trans. SNAME* 89 (1981) 397–416.
8. P. T. Pedersen, Ship grounding and hull-girder strength. *Marine Structures* 7 (1994) 1–29.
9. J. N. Newman, B. Scortland and T. Vinje, Added mass and damping of rectangular bodies close to the free surface. *J. Ship Res.* 28 (1984) 219–225.
10. D. L. Huang and Z. Zong, Hydrodynamic forces acting on a rectangular cylinder heaving close to water bottom. *Schiffstechnik* 36 (1989) 147–150.
11. J. V. Wehausen and E. V. Laitone, Surface waves. In: S. Flüsse (ed.), *Handbuch der Physik*, Band 9. Berlin: Springer-Verlag (1960) 814pp.
12. C. A. Brebbia, J. C. F. Telles and L. C. Wrobel, *Boundary Element Techniques, Theory and Applications in Engineering*. Berlin: Springer-Verlag (1984) 464pp.